RSC Advances

Graphical contents entry
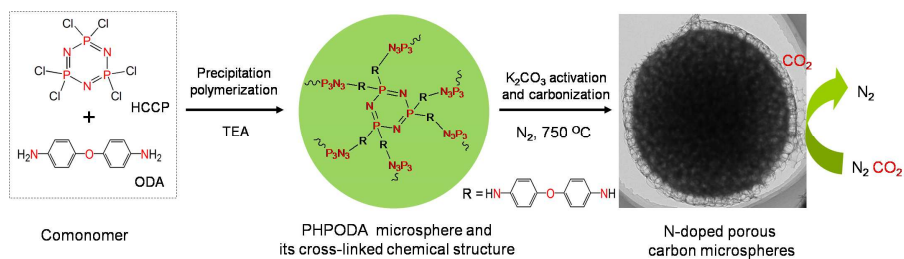
Novel carbon microspheres were synthesized from polyphosphazene and exhibit a considerable CO2 capture performance and good electrocatalytic activity for ORR.

ARTICLE TYPE

Novel N-doped porous carbon microspheres containing oxygen and phosphorus for CO_2 absorbent and metal-free electrocatalysts

Minghuan Wang, Jianwei Fu,* Jianhua Zhu, Ya Yan and Qun Xu*

Novel N-doped porous carbon microspheres were synthesized facilely from polyphosphazene. These carbons exhibit a considerable performance for CO_2 capture with high uptake, excellent selectivity, and good recyclability, and also show 10 **good electrocatalytic activity for oxygen reduction reaction.**

With the rapid development of world economics, anthropogenic CO_2 emission from the burning of fossil fuels has increased drastically over the past several decades, which is considered to be a significant contributor to global climate 15 change.[1] This opens the demand for the development of efficient materials for CO_2 capture and storage.[2, 3] Conventional CO_2 capture systems based on chemical absorption through amine solvents have major drawbacks such as the corrosion of equipment, toxicity, large energy consumption and poor material 20 stability.[4] To address these drawbacks, various porous solids as CO_2 sorbents have been investigated, including metal-organic frameworks (MOF),[5] micoporous organic polymers,[6] and porous carbons.[7] Among them, porous carbons have been under intensive study due to their low cost, availability, and high 25 moisture/chemical stabilities.[8]

Generally, the porous carbons, in which the micropores with a pore size lower than 1 nm contribute to most of the pore volume, are considered as better CO_2 adsorption-storage media,[9] and the increasing micropore specific surface area, micropore volume, 30 and well-defined micropore size distribution of porous carbons are key to achieve a better CO_2 capture capacity.[10] So considering the importance of porous carbons in practical applications, more and more intensive efforts have been focused on producing and tailoring the micro structures of porous carbons by various 35 procedures including the template method,[11] physical activation and chemical activation.[12] Among these methods, the chemical activation of various carbonaceous materials is especially suitable for forming activated porous carbons with a very high specific surface area, large pore volume, and well-defined micropore size 40 distribution (<1 nm).[10, 13] Apart from optimizing the pore structure of porous carbons, the introduction of heteroatoms such as nitrogen into the carbon framework is also promising to improve the CO_2 capture capacity and selectivity.[14, 15] Nitrogen-containing groups in porous carbons can act as Lewis basic sites 45 for anchoring acidic CO_2 molecules, thus resulting in enhanced CO_2 adsorption capacity and selectivity. Therefore, it is great interest to investigate the CO_2 capture performance of nitrogen doped porous carbons, which additionally possess very high

surface and pore volumes, and a well-defined micropore size. 50 However, many N-doped porous carbon materials have been fabricated from various polymer materials, such as polyamine[16], polypyrole[17], polyacrylonitrile,[18] and few of these porous carbons are with a high surface area and large pore volume. So it is still highly desirable to develop novel nitrogen-rich and highly porous 55 carbons from other polymer.

Herein, we use poly(hexachlorocyclotriphosphazene-co-4,4′-oxydianiline) (PHPODA) microspheres as a novel precursor, which contain plenty of nitrogen, phosphorus, and oxygen elements, and K_2CO_3 as chemical activator to prepare N-doped 60 porous carbon microspheres (N-PCMSs). Meanwhile, their CO_2 capture performance was investigated and their electrocatalytic activity for oxygen reduction reaction (ORR) was examined.

Scheme 1 illustrates the fabrication process of the N-PCMSs. Firstly, PHPODA microspheres were fabricated by directly 65 precipitation polymerization between hexachlorocyclotriphosphazene (HCCP) and 4,4′-oxydianiline (ODA), using triethylamine (TEA) as acid-acceptor in acetonitrile. Then, using PHPODA microspheres as precursor and K_2CO_3 as chemical activator, novel N-doped porous carbons 70 microspheres containing oxygen and phosphorus were prepared.
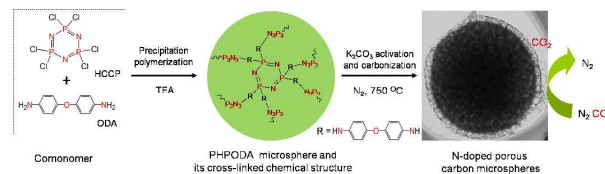
Scheme 1. Schematic illustration of the fabrication process for the N-PCMSs. N_3P_3 indicated other phosphazene cores.

Fig. 1A and 1B show SEM and TEM images of the PHPODA 75 microspheres, respectively. Obviously, the as-prepared PHPODA possess a solid structure and uniformly spherical shape with a smooth surface and an average diameter of 2.6 μm. After carbonization, the spherical morphology of the carbonized sample was retained, as shown in Fig. 1C. But a porous structure for the 80 carbonized sample was observed clearly, which might originate from mass-transfer flow during the carbonization. To deeply investigate the porous carbon microstructure, the sample was characterized by a magnified TEM image (Fig. 1D). Result reveals that large quantities of pores are homogeneously 85 dispersed within the carbon matrix. Moreover, the wall of the pores is very thin, just like 2D graphene sheet. And this structure is beneficial to the facile capture of CO_2.

To investigate the porosity of the N-PCMSs in detail, the N_2

sorption isotherm at 77 K was collected and shown in Fig. 2A. The N$_2$ adsorption-desorption isotherm for the N-PCMSs exhibits typical type-□ adsorption behavior and has a sharp uptake at P/P^0<0.1 and distinct hysteresis loops at P/P^0=0.4-1.0, indicating
5 the existence of micropore and mesopore in the N-PCMSs matrix and the N-PCMSs is a hierarchical structure. The pore size distribution analysis further proved the above conclusion, as shown in Fig. 2B. Obviously, the pore size of the N-PCMSs is predominantly distributed around 4 and 0.62 nm, respectively.
10 The textural properties of the N-PCMSs were summarized in Table S1 (ESI†). It should be noted that the N-PCMSs exhibit a high BET surface area of 1427 m^2 g^{-1} and a high total pore volume of 1.23 cm^3 g^{-1}. Especially, the surface area and pore volume of the micropore part is up to 794 m^2 g^{-1} and 0.36 cm^3 g^{-1},
15 respectively. Importantly, as Fig. 2B shows, most of the micropores have a diameter below 1 nm. This micropore structure may result in a high CO$_2$ uptake for the N-PCMSs. Other parts of the pores such as mesopores and micropores (> 1 nm) may effect the CO$_2$ adsorption capacity less but enhance the gas
20 transportation for better CO$_2$ accessibility to the micropores where gas is mainly captured, thus facilitate diffusion and adsorption of CO$_2$ molecules.[19] Therefore such textural properties favor the CO$_2$ capture for the N-PCMSs.
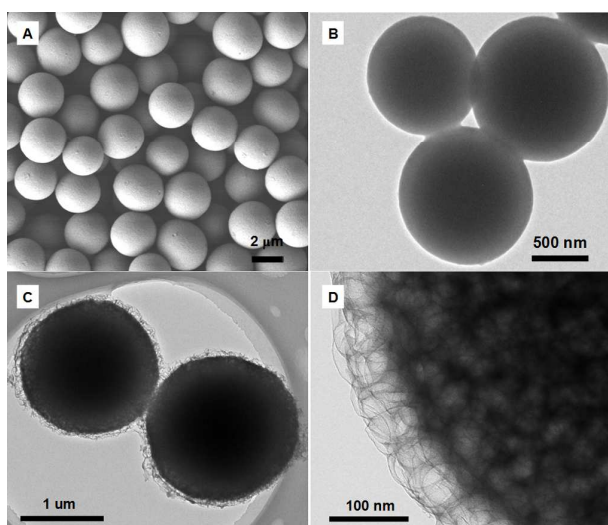

25 **Fig. 1** (A) SEM and (B) TEM images for PHPODA microspheres. (C, D) TEM images with different magnification for the N-PCMSs.
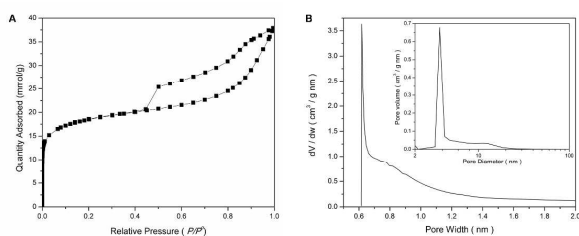

Fig. 2 The nitrogen adsorption - desorption isotherms at 77 K (A)
30 and the pore size distribution of micropores (B) by H-K method for the N-PCMSs. (inset: the pore size distribution of mesopores.)

In addition, XPS was performed to further investigate the surface states of the N-PCMSs. The XPS survey spectrum of the N-PCMSs is shown in Fig. 3A, and it exhibits four typical speaks
35 assigned to C1s, N1s, O1s, and P2p respectively. As Fig. 3B shows, the N1s peak can be resolved into four individual component peaks representing N-6 (398.5 eV), N-5 (400.0 eV), N-Q (401.2 eV), and N-X (403.0 eV) groups. The peak at 400.0

eV corresponds to N atoms trigonally bonded with sp^2 or sp^3 C
40 atoms. And the peak at 398.5 eV can be assigned to sp^2 N atoms bonded to carbon atoms.[20, 21] It should be stressed here N - 6 and N - Q peaks do not just correspond to pyridinic and quaternary N but also to the remaining P = N and P - N bonds.[22-24] It is worth to note that in the N-PCMSs, the pyrrolic gourps (N-5) are the
45 main type of N-functionalities, which give Lewis basicity to the materials and exhibit the highest influence on CO$_2$ capture among the nitrogen functional groups.[25, 26] The C1s peak also can be resolved into six individual component peaks at 284.6, 285.4, 286.3, 287.5, 288.8 and 289.0 eV (Fig. S1, ESI†). It is obvious
50 that the major peak is at 284.6 eV, which can be assigned to pure graphitic C=C species.[27, 28] The higher peak at 285.4 eV is corresponding to C=C localized bonds.[29] The peak at 286.3 eV is not only assigned to sp^3 carbon species, but also to C-O bonds in in ether, phenol and anhydride functional groups and C-N bonds
55 in aromatic rings.[30, 31] Moreover, the signals of the C-O-P, C-P and C-P=O linkages in the case of phosphorus-containing samples are also detected at around 286 eV, thus they could appear in this peak.[32] The peak at 287.5 eV is attributed to C=O and C=N bonds and the π→π* shake up peak of band centered at
60 285.4 eV. The peak at 288.8 eV is assigned to C-O bonds in carboxyl and ester groups and nitrogen component.[29, 32] The highest peak at 290.0 eV is contributed to the π→π* shake up peak of band centered at 284.6 eV.[29, 31] These assignments are consistent with the N1s spectrum. These results are further
65 confirmed by the FTIR spectrum (Fig. S2, ESI†). In addition, element analysis shows the corresponding content of each elements (C, N, O, and P) is 83.02, 3.65, 11.64, and 1.16 at.% respectively, indicating that a significant number of nitrogen atoms are bonded to C atoms and numerous O and P are remained
70 in the N-PCMSs. The exist of amount of nitrogen atoms in the carbons will be beneficial to the CO$_2$ adsorption for the N-PCMSs. Although the presence of numerous oxygen and phosphorus atoms may be detrimental for the CO$_2$ adsorption for their groups as acidic ones toward adsorption of CO$_2$ molecules,
75 especially at a high temperature,[26] the oxygen-containing groups such as oxygen-containing ether and hydroxyl groups can also interact with CO$_2$ molecules via electrostatic interactions leading to enhanced CO$_2$ capture capacity and developed CO$_2$ selectivity.[33-35]

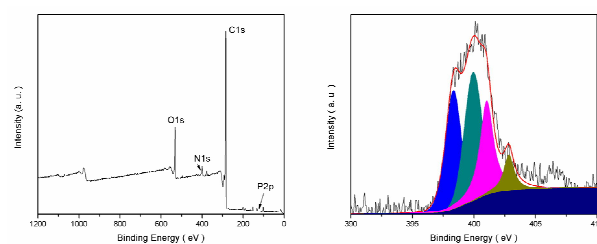80 Fig. 3 The XPS spectra of the N-PCMSs: (A) survey spectrum and (B) N1s spectrum.

XRD pattern for the N-PCMSs is shown in Fig. S3 (ESI†). There are two broad peaks at 2θ values of around 25 and 43°,
85 which can be assigned to (002) and (100) planes of graphite carbon materials respectively.[36, 37] The broad diffraction peaks indicate that no pronounced graphitization occurred during the pyrolysis process. Also, the Raman spectrum of the N-PCMSs further confirmed the above conclusion (Fig. S4, ESI†). It
90 exhibits two broad and strong bands at about 1590 and 1347 cm^{-1}, corresponding to the in-plane bond-stretching motion of the pairs of C-sp^2 atoms and the disorder-induced mode associate with structure defects and imperfections, respectively.[38, 39] The ratio of D and G bands (I_D/I_G) for N-PCMSs calculated is 0.96,

suggesting the low graphitized degree of the N-PCMSs.

Fig. 4A shows the CO_2 sorption isotherms of the N-PCMSs at different temperature. It indicates that the N-PCMSs have a much higher performance for CO_2 capture with a capacity of 5.7 mmol g^{-1} at 273 K and 1.0 bar. Moreover, the CO_2 uptake of the N-PCMSs is still up to 3.8 mmol g^{-1} at 298 K and 1.0 bar, indicating that the CO_2 capture capacities of the N-PCMSs reported here are among the highest ever reported for porous carbons. This is evidenced by comparing our CO_2 uptake data with that of other porous carbon materials reported in recent work, which are shown in Table 1. In addition, it is important that there is no saturation observed up to a pressure of 1.0 bar, which indicates a higher CO_2 adsorption capacity can be achieved at a higher pressure. This high CO_2 adsorption amount could be attributed to the high surface area, especially the large part of micropores, and the high nitrogen content of the N-PCMSs. This result is strongly supported by the fact that the isosteric heat of CO_2 adsorption, calculated by means of the Clausius–Clapeyron equation from the CO_2 adsorption-desorption isotherms of the N-PCMSs at two temperatures (*i.e.*, 273 and 298 K). The isosteric heat of adsorption decreases from 41 to 23 kJ mol^{-1} as the CO_2 adsorption amount increases from 0.2 to 3.8 mmol g^{-1} (Fig. S5 ESI†). The high initial isosteric heat of adsorption is mainly due to the amine groups that serve as Lewis bases and readily interact with the acidic CO_2 molecules, and this is consistent with previous studies.[40] This also suggests that the large CO_2 uptake by the N-PCMSs is due to a synergistic effect of the narrow microporosity and the large number of N functional groups.
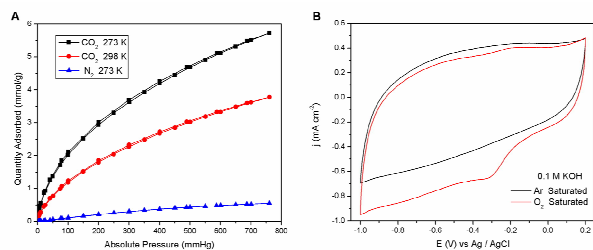

Fig. 4 (A) The gas adsorption isotherms of the N-PCMSs at different temperature. (B) The cyclic voltammetry curves of oxygen reduction reactions on N-PCMSs in Ar- (black) and oxygen- (red) saturated 0.1 M KOH electrolyte solution.

Table 1 Comparison of CO_2 uptakes at 1.0 bar for different carbon sorbents

Sample	CO_2 uptake /mmol g^{-1}		Selectivity	Ref.
	273 K	298 K		
HTC-K1-T8	4.9	3.0	--	41
NPC-650	5.27	3.1	6.6 (273 K)	42
AS-2-600	6.1	4.8	5.4 (298 K)	43
N-PCMSs	5.7	3.8	10 (273 K)	This work
AC-2–635	5.9	3.86	21 (298 K)	44

To evaluate the CO_2 separation performance of the N-PCMSs, single component CO_2 and N_2 sorption isotherms are collected at 273 K (Fig. 4A). Comparatively, the absorption capacity of the N-PCMSs for N_2 is only 0.55 mmol g^{-1} at 273 K and 1.0 bar, which is below 10% of the value for CO_2 at the same temperature. This suggests the N-PCMSs have a high selectivity for CO_2 over N_2.(Table 1) Furthermore, as shown in Fig. S6 (ESI†), the selectivity has the tendency of increase with the pressure decreasing, and it is up to around 50 at the initial adsorption, which is higher than those previously reported values of other porous carbons.[8, 19, 45] The result indicates that the N-PCMSs are potential selective sorbents for CO_2 and N_2 separation, highly advantageous for practical applications.

The recycling performance of the N-PCMSs as CO_2 adsorbent was examined by performing the adsorption - desorption cycle for several times at 273 K. As shown in Fig. S7 (ESI†), no evidence decrease in the CO_2 uptake for the adsorption-desorption cycle after five cycles is observed and all the adsorption capacities of the CO_2 are still around 5.7 mmol g^{-1} at 1 bar, indicating that the N-PCMSs are highly stable CO_2 capture sorbents and possess good recyclability toward CO_2.

In addition, it is well known that the N-doped carbons have electrochemical activity as metal free catalyst for oxygen reduction reaction (ORR).[46, 47] So the electrocatalystic activity of the N-PCMSs for ORR was tested by cyclic voltammetry (CV) in an Ar or O_2 saturated 0.1 M KOH solution at a scan rate of 100 mV s^{-1}. As shown in Fig. 4B, there was not any obvious peak observed in the Ar saturated solution. In contrast, it is clearly seen that a well-defined cathodic ORR peak at -0.3 V with a high reaction current of -0.64 mA cm^{-2} occurred in the CV analysis when the electrolyte solution was saturated with O_2. This indicates that the N-PCMSs have a pronounced electrocatalytic activity toward ORR.

In summary, the N-PCMSs were prepared facilely using PHPODA as precursor and K_2CO_3 as activator in this study. Results show that as-prepared N-PCMSs have a high surface area of 1427 m^2 g^{-1}, a large pore volume of 1.23 cm^3 g^{-1}, and a nitrogen content of 3.65 at.%. Importantly, the micropore surface area is up to 794 m^2 g^{-1}, and the micropore size is mostly below 1 nm. The N-PCMSs have achieved a remarkable performance for CO_2 capture and the CO_2 uptake is up to 5.7 and 3.7 mmol g^{-1} at 273 and 298 K respectively. Moreover, these porous carbons show an excellent selectivity for CO_2/N_2 separation and good regeneration ability. In addition, the N-doped porous carbons also exhibit good electrocatalytic activity for oxygen reduction reaction. Further application of the novel N-PCMSs with different nitrogen content as high-surface-area electrode materials is currently underway.

Notes and references

School of Materials Science and Engineering, Zhengzhou University, Zhengzhou, P. R. China. Fax: +86-371-67767827; Tel: +86-371-67767827; E-mail: jwfu@zzu.edu.cn; qunxu@zzu.edu.cn
† Electronic Supplementary Information (ESI) available: Detailed synthetic processes and additional characterization available. See DOI: 10.1039/b000000x/

1   K. J. van Groenigen, C. W. Osenberg and B. A. Hungate, *Nature*, 2011, **475**, 214.
2   K. S. Lackner, *Science*, 2003, **300**, 1677.
3   D. M. D'Alessandro, B. Smit and J. R. Long, *Angew. Chem. Int. Edit.*, 2010, **49**, 6058.
4   D. Aaron and C. Tsouris, *Sep. Sci. Technol.*, 2005, **40**, 321.
5   S. Yang, X. Lin, W. Lewis, M. Suyetin, E. Bichoutskaia, J. E. Parker, C. C. Tang, D. R. Allan, P. J. Rizkallah, P. Hubberstey, N. R. Champness, K. Mark Thomas, A. J. Blake and M. Schröder, *Nat. Mater.*, 2012, **11**, 710.

6   N. Du, H. B. Park, G. P. Robertson, M. M. Dal-Cin, T. Visser, L. Scoles and M. D. Guiver, *Nat. Mater.*, 2011, **10**, 372.
7   W. Shen and W. Fan, *J. Mater. Chem. A*, 2013, **1**, 999.
8   V. Chandra, S. U. Yu, S. H. Kim, Y. S. Yoon, D. Y. Kim, A. H. Kwon, M. Meyyappan and K. S. Kim, *Chem. Commun.*, 2012, **48**, 735.
9   V. Presser, J. McDonough, S. Yeon and Y. Gogotsi, *Energy Environ. Sci.*, 2011, **4**, 3059.
10 J. Wang and S. Kaskel, *J. Mater. Chem.*, 2012, **22**, 23710.
11 J. Lee, J. Kim and T. Hyeon, *Adv. Mater.*, 2006, **18**, 2073.
12 M. Sevilla and R. Mokaya, *Energy Environ. Sci.*, 2014, **7**, 1250.
13 T. Otowa, R. Tanibata and M. Itoh, *Gas Separation & Purification*, 1993, **7**, 241.
14 Y. Xia, Y. Zhu and Y. Tang, *Carbon*, 2012, **50**, 5543.
15 G. Hao, W. Li, D. Qian, G. Wang, W. Zhang, T. Zhang, A. Wang, F. Schu·th, H. Bongard and A. Lu, *J. Am. Chem. Soc.*, 2011, **133**, 11378.
16 D. Lin, X. Zhang, X. Cui and W. Chen, *RSC Adv.*, 2014, **4**, 27414.
17 M. Sevilla, P. Valle-Vigón and A. B. Fuertes, *Adv. Funct. Mater.*, 2011, **21**, 2781.
18 W. Shen, S. Zhang, Y. He, J. Li and W. Fan, *J. Mater. Chem.*, 2011, **21**, 14036.
19 D. Lee, C. Zhang, C. Wei, B. L. Ashfeld and H. Gao, *J. Mater. Chem. A*, 2013, **1**, 14862.
20 A. Vinu, *Adv. Funct. Mater.*, 2008, **18**, 816.
21 A. Vinu, K. Ariga, T. Mori, T. Nakanishi, S. Hishita, D. Golberg and Y. Bando, *Adv. Mater.*, 2005, **17**, 1648.
22 D. Hulicova-Jurcakova, M. Seredych, G. Q. Lu, N. K. A. C. Kodiweera, P. E. Stallworth, S. Greenbaum and T. J. Bandosz, *Carbon*, 2009, **47**, 1576.
23 C. Wang, L. Sun, Y. Zhou, P. Wan, X. Zhang and J. Qiu, *Carbon*, 2013, **59**, 537.
24 W. B. Perry, T. F. Schaaf and W. L. Jolly, *J. Am. Chem. Soc.*, 1975, **97**, 4899.
25 M. Sevilla, C. Falco, M. Titirici and A. B. Fuertes, *RSC Adv.*, 2012, **2**, 12792.
26 A. Sánchez-Sánchez, F. Suárez-García, A. Martínez-Alonso and J. M. D. Tascón, *ACS Appl. Mater. Interfaces.*, 2014, **6**, 21237.
27 Q. Li, J. Yang, D. Feng, Z. Wu, Q. Wu, S. S. Park, C. Ha and D. Zhao, *Nano Res.*, 2010, **3**, 632.
28 A. Sánchez-Sánchez, F. Suárez-García, A. Martínez-Alonso and J. M. D. Tascón, *Carbon*, 2013, **62**, 193.
29 A. Sánchez-Sánchez, F. Suárez-García, A. Martínez-Alonso and J. M. D. Tascón, *Appl. Surf. Sci.*, 2014, **299**, 19.
30 A. B. Dongil, B. Bachiller-Baeza, A. Guerrero-Ruiz, I. Rodriguez-Ramos, A. Martinez-Alonso and J. M. Tascon, *J. Colloid. Interface Sci.*, 2011, **355**, 179.
31 J. I. Paredes, S. Villar-Rodil, P. Solís-Fernández, A. Martínez-Alonso and J. M. D. Tascón, *Langmuir*, 2009, **25**, 5957.
32 A. M. Puziy, O. I. Poddubnaya, R. P. Socha, J. Gurgul and M. Wisniewski, *Carbon*, 2008, **46**, 2113.
33 Y. Liu and J. Wilcox, *Environ. Sci. Technol.*, 2013, **47**, 95.
34 Y. Luo, B. Li, W. Wang, K. Wu and B. Tan, *Adv. Mater.*, 2012, **24**, 5703.
35 R. Babarao, S. Dai and D. Jiang, *Langmuir*, 2011, **27**, 3451.
36 L. Zhang, M. Zhang, Y. Wang, Z. Zhang, G. Kan, C. Wang, Z. Zhong and F. Su, *J. Mater. Chem. A*, 2014, **2**, 10161.
37 Y. Wang, F. Su, C. D. Wood, J. Y. Lee and X. S. Zhao, *Ind. Eng. Chem. Res.*, 2008, **47**, 2294.
38 W. Chen, R. B. Rakhi, L. Hu, X. Xie, Y. Cui and H. N. Alshareef, *Nano Lett.*, 2011, **11**, 5165.
39 S. Lee, S. Bak, C. Lee, C. Jaye, D. A. Fischer, B. Kim, X. Yang, K. Nam and K. Kim, *J. Phys. Chem. C*, 2014, **118**, 2834.
40 J. Wei, D. Zhou, Z. Sun, Y. Deng, Y. Xia and D. Zhao, *Adv. Funct. Mater.*, 2013, **23**, 2322.
41 F. J. Martín-Jimeno, F. Suárez-García, J. I. Paredes, A. Martínez-Alonso and J. M. D. Tascón, *Carbon*, 2015, **81**, 137.
42 J. Wang, I. Senkovska, M. Oschatz, M. R. Lohe, L. Borchardt, A. Heerwig, Q. Liu and S. Kaskel, *J. Mater. Chem. A*, 2013, **1**, 10951.
43 M. Sevilla and A. B. Fuertes, *Energy Environ. Sci.*, 2011, **4**, 1765.
44 X. Fan, L. Zhang, G. Zhang, Z. Shu and J. Shi, *Carbon*, 2013, **61**, 423.
45 S. Feng, W. Li, Q. Shi, Y. Li, J. Chen, Y. Ling, A. M. Asiri and D. Zhao, *Chem. Commun.*, 2014, **50**, 329.
46 R. Liu, H. Liu, Y. Li, Y. Yi, X. Shang, S. Zhang, X. Yu, S. Zhang, H. Cao and G. Zhang, *Nanoscale*, 2014, **6**, 11336.
47 X. Wang, J. Wang, D. Wang, S. Dou, Z. Ma, J. Wu, L. Tao, A. Shen, C. Ouyang, Q. Liu and S. Wang, *Chem. Commun.*, 2014, **50**, 4839.